ISTITUTO NAZIONALE DI FISICA NUCLEARE
Laboratori Nazionali di Frascati

LNF-81/40(R)
8 Luglio 1981

V. Bellini, R. Caloi, L. Casano, M. P. De Pascale, M. Di Toro, V. Emma, S. Frullani, G. Giordano, B. Girolami, S. Lo Nigro, G. Matone, M. Mattioli, C. Milone, G. S. Pappalardo, P. Picozza, E. Poldi, D. Prosperi and C. Schaerf: FISSION OF EVEN-EVEN NUCLEI BY MONOCHROMATIC POLARIZED LADON PHOTON BEAM IN FRASCATI.

Servizio Documentazione
dei Laboratori Nazionali di Frascati
Cas. Postale 13 - Frascati (Roma)

INFN - Laboratori Nazionali di Frascati
Servizio Documentazione

LNF-81/40(R)
8 Luglio 1981

FISSION OF EVEN-EVEN NUCLEI BY MONOCHROMATIC POLARIZED LADON PHOTON BEAM IN FRASCATI

V. Bellini, M. Di Toro, V. Emma, S. Lo Nigro, C. Milone, G. S. Pappalardo
INFN - Sezione di Catania, and Istituto di Fisica dell'Università di Catania

The LADON Group:

M. P. De Pascale, G. Giordano, G. Matone, P. Picozza
INFN - Laboratori Nazionali di Frascati

R. Caloi, L. Casano, M. Mattioli, E. Poldi, D. Prosperi, C. Schaerf
INFN - Sezione di Roma

S. Frullani, B. Girolami
INFN - Sezione Sanità.

1. - INTRODUCTION.

The low energy photofission of nuclei has been studied, up to now, by using photon sources obtained by electron bremsstrahlung[1-9] or by radiative neutron capture in selected elements[10-13] or by positron annihilation in flight[14]. Each of such beams presents characteristics which often limit its use and make very hard the experimental data analysis.

In this paper we show the improvements that can be attained in performing photofission experiments at energies $E_\gamma \leq 10$ MeV by using the monochromatic and polarized photon beam available at the Frascati Laboratories.

The photofission study at photon energy $E_\gamma \leq 10$ MeV is very interesting because it permits to deduce information on the levels in the transition state nucleus and on the structure of the potential barrier at the scission point. Such information is generally deduced by the analysis of photofission cross-section and fragment angular distributions measured at different excitation energies near the fission threshold.

The photofission of even-even actinide nuclei is a very simple case because the low-energy photon absorption occurs through electric dipole and quadrupole processes which produce com-

pound-nucleus states only with $J = 1^-, 2^+$.

The photofission cross-section in the giant dipole resonance (GRD) region has been widely studied by using different photon beams and different fragment detection techniques (see Caldwell et al.[14], and references therein).

The experimental data for ^{238}U and other actinide nuclei at photon energies from fission threshold up to $E_\gamma = 9$ MeV show discrepancies both on the behaviour and on the absolute values, as clearly evidenced in Fig. 10 of ref. (14).

The angular distributions of fission fragments, measured by unpolarized photon beams[5,10,11], have permitted to deduce information only for three low-energy fission channels in the transition state of the nucleus. Up to now the presence of the $(K, J) = (0, 2^+)$, $(0, 1^-)$ and $(1, 1^-)$ channels has been observed. K is the J-projection on the nuclear symmetry axis.

In a recent experiment[15] on the electrofission and photofission of ^{238}U a more significant electric quadrupole contribution in the 6-9 MeV energy region has been suggested; this contribution cannot be clearly seen in an angular distribution analysis using the conventional photon beams.

A significant improvement in the information on the fission channels can be obtained by using a monochromatic and polarized photon beam, as demonstrated by some of us in a previous work[16].

The advantages attained in performing photofission experiments with a polarized photon beam are described in Sect. 2.

A photon beam with the required characteristics is at present available at the Frascati National Laboratories (LADON facility[17]).

The main characteristics of this photon beam are described in Sect. 3.

The experimental technique for the measurements of photofission cross-section and angular distribution is reported in Sect. 4.

2. - FRAGMENT ANGULAR DISTRIBUTIONS.

The energy levels of a fissioning nucleus in the transition state are characterized by the quantum numbers J (total angular momentum), K (projection of J on the nuclear symmetry axis), M (component of J along a space-fixed x axis, for example the incident beam direction) and the parity π. In the low-energy photofission of even-even nuclei, compound-nucleus states with $J = 1^-, 2^+$ and $M = \pm 1$ are excited.

Assuming that the fission fragments are emitted along the nuclear symmetry axis, the fragment angular distribution depends on the probability distribution of the symmetry axis direction. Such a distribution has been calculated by Wheeler[18] and, in the case of fission induced on even-even nuclei by unpolarized photons, is expressed in the following form:

$$W_K^J(\theta) = \frac{2J+1}{4} \left[\left| d^J_{1,K}(\theta) \right|^2 + \left| d^J_{-1,K}(\theta) \right|^2 \right] \qquad (1)$$

where $d^J_{M,K}$ are real functions of θ (the angle of fragment emission with respect to the beam di-

rection) and are defined in ref. (18).

In the absence of polarization in the incident beam, the fragment distribution in a plane perpendicular to the z-axis (azimuthal distribution) is isotropic because all azimuths of J about this axis are equally likely.

By using a linearly polarized photon beam, we have shown[16] that the fragment angular distribution in the fission of even-even nuclei, is given by:

$$W_K^J(\theta,\varphi) = \frac{2J+1}{2}\left\{\frac{1}{2}\left[\left|d^J_{1,K}(\theta)\right|^2 + \left|d^J_{-1,K}(\theta)\right|^2\right] + P\cos 2\varphi\, d^J_{1,K}(\theta)\, d^J_{-1,K}(\theta)\right\} \qquad (2)$$

where P is the photon polarization degree and φ is the azimuthal angle measured with respect to the polarization direction. In the case P = 0, eq. (2) gives eq. (1); in the case P = 1 (highly polarized photon beam), eq. (2) clearly indicates that the fragment distribution is strongly dependent on the azimuthal angle φ.

Till now the analysis of the experimental angular distributions in photofission of ^{238}U and other even-even nuclei[5, 10, 11] has permitted to deduce information only on three fission channels characterized by the quantum numbers $(K, J) = (0, 2^+)$, $(0, 1^-)$ and $(1, 1^-)$.

Using the extra information supplied by the new degree of freedom related to the polarization direction, we can try to get more data on the fission mechanism. In particular we can try to disentangle the behaviour of a larger number of fission channels.

At low energies $E_\gamma \lesssim 9$ MeV, we are looking for the following five channels: $(K, J) = (0, 1^-)$, $(0, 2^+)$, $(\pm 1, 1^-)$, $(\pm 1, 2^+)$, $(\pm 2, 2^+)$.

The azimuthal distributions $W_K^J(\pi/2, \varphi)$ and $W_K^J(\pi/4, \varphi)$, expected for the considered five channels, are reported in Figg. 1a and 1b, respectively.

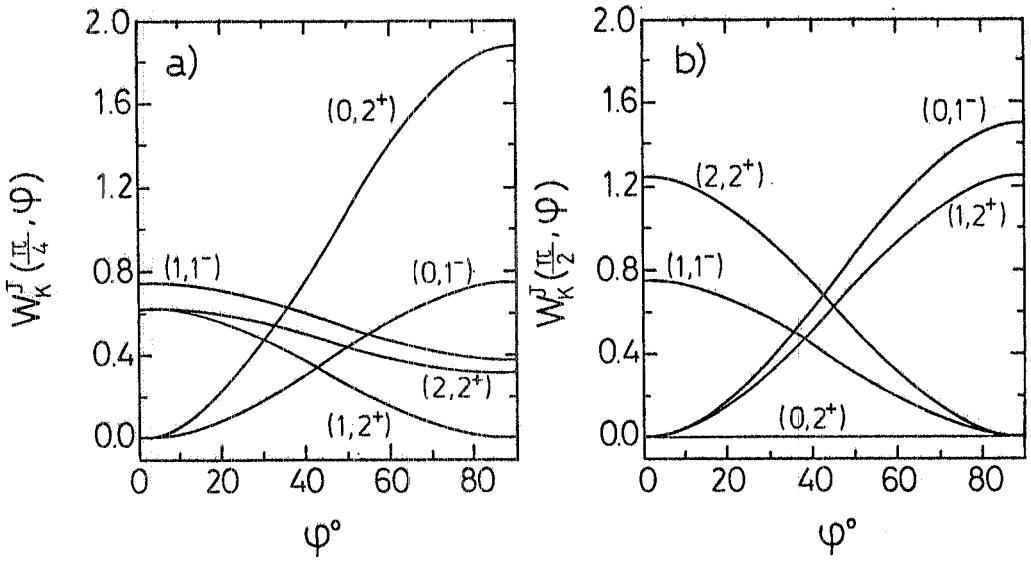

FIG. 1 - Fragment azimuthal distributions in the fission induced on even-even nuclei by totally polarized photons. a) Distributions $W_K^J(\pi/4, \varphi)$; b) Distributions $W_K^J(\pi/2, \varphi)$.

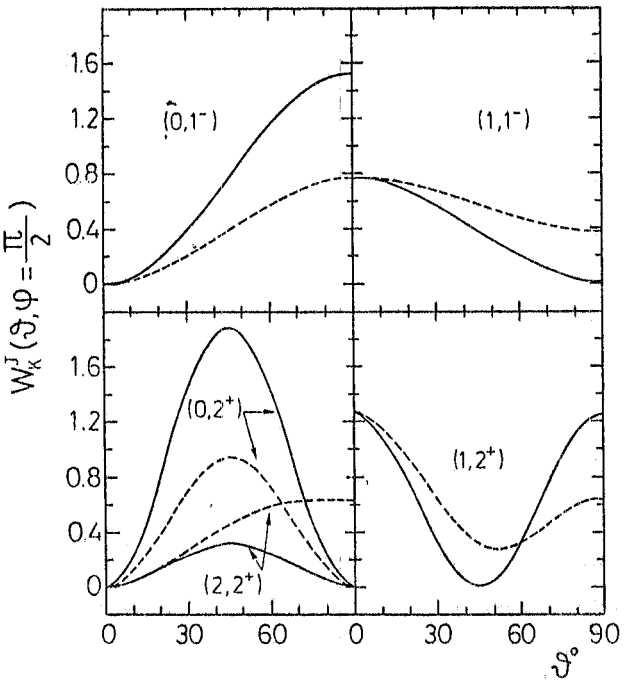

FIG. 2 - Fragment angular distributions $W_K^J(\theta, \pi/2)$ in the fission induced by photons on even-even nuclei. The continuous curves are obtained for P = 1, the dashed ones for P = 0.

The angular distributions $W_K^J(\theta, \pi/2)$ expected for the same five channels and calculated for P = 1 (continuous curves) and P = 0 (dashed curves) respectively, are reported in Fig. 2.

Comparing Fig. 1a and 1b we observe that the azimuthal distribution $W_K^J(\pi/2, \varphi)$ for the $(0, 2^+)$ channel is identically zero; on the contrary, for the same channel, the distribution $W_K^J(\pi/4, \varphi)$ is strongly increasing. In Fig. 2 we can also deduce that in the case of the $(0, 2^+)$ channel excitation we have for P = 1 and $\varphi = \pi/2$ an angular distribution that is twice the one obtained for P = 0. As a consequence, we can better observe such a state by measuring the $W(\pi/4, \varphi)$ and $W(\theta, \pi/2)$ distributions by means of highly polarized photon beams.

The analytical expressions of the azimuthal and angular distributions, plotted in Figg. 1 and 2 are collected in Table I.

TABLE I - Analytical expressions of the azimuthal and angular distributions of fission fragments of even-even nuclei for individual dipole and quadrupole channels.

Channel (K, J^π)	$W_K^J(\theta, \frac{\pi}{2})$	$W_K^J(\frac{\pi}{2}, \varphi)$	$W_K^J(\frac{\pi}{4}, \varphi)$
$(0, 1^-)$	$\frac{3}{4}(\sin^2\theta + P \sin^2\theta)$	$\frac{3}{4} - \frac{3}{4}P(1 - 2\sin^2\varphi)$	$\frac{3}{8}(1 - P) + \frac{3}{4}P \sin^2\varphi$
$(\pm 1, 1^-)$	$\frac{3}{4}(1 - \frac{1}{2}\sin^2\theta) - \frac{3}{8}P \sin^2\theta$	$\frac{3}{8} + \frac{3}{8}P(1 - 2\sin^2\varphi)$	$\frac{3}{16}(3+P) - \frac{3}{8}P \sin^2\varphi$
$(0, 2^+)$	$\frac{15}{16}(\sin^2 2\theta + P \sin^2 2\theta)$	$\equiv 0$	$\frac{15}{16}(1 - P) + \frac{15}{8}P \sin^2\varphi$
$(\pm 1, 2^+)$	$\frac{5}{8}(2 - \sin^2\theta - \sin^2 2\theta) - \frac{5}{8}P(\sin^2 2\theta - \sin^2\theta)$	$\frac{5}{8} - \frac{5}{8}P(1 - \sin^2\varphi)$	$\frac{5}{16}(1+P) - \frac{5}{8}P \sin^2\varphi$
$(\pm 2, 2^+)$	$\frac{5}{8}(\sin^2\theta + \frac{1}{4}\sin^2 2\theta) - \frac{5}{8}P(\sin^2\theta - \frac{1}{4}\sin^2 2\theta)$	$\frac{5}{8} + \frac{5}{8}P(1 - 2\sin^2\varphi)$	$\frac{5}{32}(3+P) - \frac{5}{16}P \sin^2\varphi$

The improvement on the obtainable information on the fission-channels, consists in the fact that at least four channels can be analysed with polarized photons, by considering the distributions $W(\theta, \pi/2)$ (angular distribution in a plane perpendicular to the polarization direction of photons)

and $W(\pi/4, \varphi)$ (azimuthal distributions of the fragments emitted at $\theta = \pi/4$).

If all five considered channels are involved in the reaction, the total distributions $W(\theta, \pi/2)$, $W(\pi/4, \varphi)$ can be written as

$$\begin{aligned} W(\theta, \pi/2) &= \sigma_{0,2} W_0^2(\theta, \pi/2) + \sigma_{0,1} W_0^1(\theta, \pi/2) + \sigma_{1,1} W_1^1(\theta, \pi/2) + \sigma_{1,2} W_1^2(\theta, \pi/2) + \\ &+ \sigma_{2,2} W_2^2(\theta, \pi/2) = a + b \sin^2\theta + c \sin^2 2\theta \,, \\ W(\pi/4, \varphi) &= \sigma_{0,2} W_0^2(\pi/4, \varphi) + \sigma_{0,1} W_0^1(\pi/4, \varphi) + \sigma_{1,1} W_1^1(\pi/4, \varphi) + \sigma_{1,2} W_1^2(\pi/4, \varphi) + \\ &+ \sigma_{2,2} W_2^2(\pi/4, \varphi) = A + B \sin^2\varphi \,, \end{aligned} \tag{3}$$

where the coefficients $\sigma_{K,J}$ are proportional to the cross-sections for photofission through the corresponding channels, and W_K^J have the analytical expression reported in Table I.

Thus, the following system of linear equations for the $\sigma_{K,J}$ unknowns is obtained:

$$\begin{aligned} a &= \frac{3}{4}\sigma_{1,1} + \frac{5}{4}\sigma_{1,2} \,, \\ b &= \frac{3}{4}(1+P)\sigma_{0,1} - \frac{3}{8}(1+P)\sigma_{1,1} - \frac{5}{8}(1-P)\sigma_{1,2} + \frac{5}{8}(1-P)\sigma_{2,2} \,, \\ c &= \frac{15}{16}(1+P)\sigma_{0,2} - \frac{5}{8}(1+P)\sigma_{1,2} + \frac{5}{32}(1+P)\sigma_{2,2} \,, \\ A &= \frac{3}{8}(1-P)\sigma_{0,1} + \frac{3}{16}(3+P)\sigma_{1,1} + \frac{15}{16}(1-P)\sigma_{0,2} + \frac{5}{16}(1+P)\sigma_{1,2} + \frac{5}{32}(3+P)\sigma_{2,2} \,, \\ B &= P\left(\frac{3}{4}\sigma_{0,1} - \frac{3}{8}\sigma_{1,1} + \frac{15}{8}\sigma_{0,2} - \frac{5}{8}\sigma_{1,2} - \frac{5}{16}\sigma_{2,2}\right) . \end{aligned} \tag{4}$$

From the best-fits of the experimental distributions $W(\theta, \pi/2)$ and $W(\pi/4, \varphi)$ we determine the parameters a, b, c, A and B.

In the case of unpolarized photon beams, we can measure only the angular distribution $W_K^J(\theta)$ from which the coefficients a, b and c can be determined and then is not possible to analyse more than three fission channels.

On the contrary, in the case of measurements with polarized photons, we obtain the system (4) the matrix of which has rank equal to 4, consequently we can analytically deduce the contributions of at least four channels.

At photon energies we are analysing, the excitation of the $(0, 2^+)$, $(0, 1^-)$, $(1, 1^-)$ channels has been ascertained. In order to identify the fourth channel among the five considered (it is possible to estimate the contribution solving the system (4)), we can analyse the behaviour of the angular distribution measured for $\varphi = 0$. In fact the $W_K^J(\theta, 0)$ distributions, valued for $P = 1$ and drawn in Fig. 3, indicate that the contribution coming from the channel $(1, 2^+)$ is strongly different from that of the $(2, 2^+)$ channel.

Moreover we want to remark that an improvement in the information on the fission channels can be obtained by using polarized photons also in the case where only three channels are excited. That is shown in appendix.

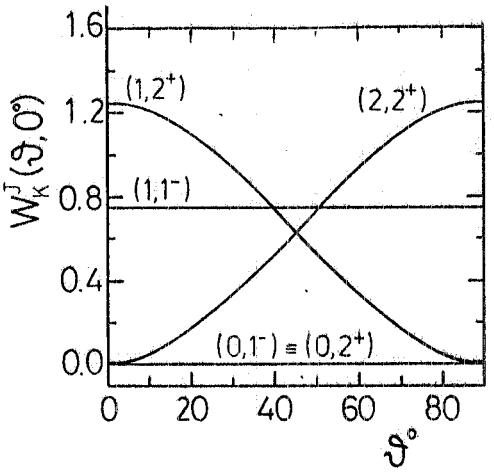

FIG. 3 - Fragment angular distributions $W_K^J(\theta, \varphi=0^\circ)$ in the fission induced on even-even nuclei by totally polarized photons.

3. - PHOTON BEAM.

The monoenergetic and polarized LADON photon beam is produced at the Frascati National Laboratories by backward Compton scattering of Laser light on high energy electrons. An Argon Ion Laser (λ = 5145 Å) and the electron storage ring Adone ($E_{e_{max}}$ = = 1.5 GeV) are used.

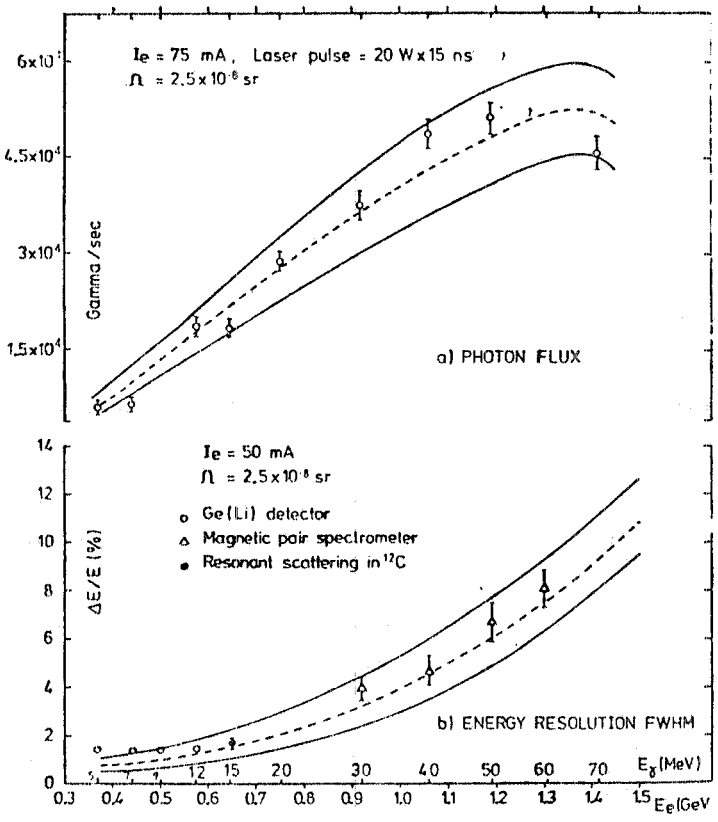

FIG. 4 - a) Photon flux; b) Fractional energy resolution (Full width half maximum). The dashed lines have been obtained by a Monte-Carlo calculation with the best estimates of the electron beam parameters. The solid lines delimit the uncertainty we have in the knowledge of these parameters.

The main characteristics of the γ-ray beam are[17]:

a) a photon energy continuously adjustable between ~ 5 MeV and ~78 MeV, for an electron energy ranging from 0.37 GeV to 1.5 GeV;

b) a beam intensity between ~ 10^4 and ~ 10^5 photons/sec, depending on electron energy, electron current, Laser power and photon energy resolution;

c) an energy resolution between ~ 1 % and ~ 10 %;

d) an almost total linear polarization (P ≃ 1);

e) a low background of photons of different energy.

The photon intensity measured with a NaI(T1) detector and a Lead Glass Cerenkov counter is reported in Fig. 4. The experimental results have been obtained for an electron current I_e = 75 mA, a Laser energy per pulse of 3×10^{-7} J (20 W x 15 ns)

and an acceptance solid angle of 2.5×10^{-8} sr. The dashed line in Fig. 4 has been obtained by a Monte-Carlo calculation with the best estimates of the electron beam parameters, the solid lines delimit the uncertainty we have in the knowledge of these parameters.

The beam energy resolution has been measured with a Ge(Li) detector for γ-ray energies up to 12 MeV and with a 180° pair spectrometer for photon energies higher than 30 MeV. At 15.1 MeV an indirect measurement of the energy resolution has been obtained by the resonant scattering of photons on ^{12}C. The experimental data are reported in Fig. 4.

Fig. 5 shows the comparison between an experimental photon spectrum at $E_\gamma \simeq 78$ MeV, obtained with the spectrometer after bremsstrahlung subtraction, an the corresponding Monte-Carlo calculation.

The polarization of the γ-ray has been verified by a scattering experiment of 15.1 MeV photons from a ^{12}C target and by an experiment on deuteron photodisintegration[17]. The results of the polarization degree P of the photon beam are 0.99 ± 0.02 and 0.97 ± 0.06 respectively. The two measures agree with the theoretically predicted value of ~ 0.999.

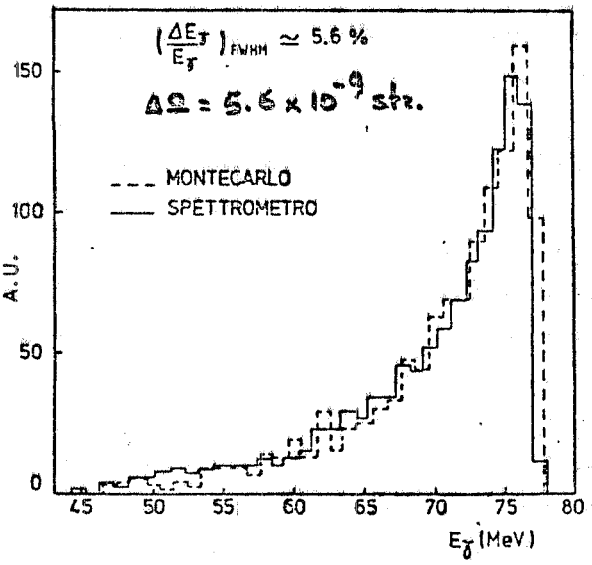

FIG. 5 - Experimental photon spectrum obtained at $E_\gamma \simeq 78$ MeV with the pair spectrometer compared with a Monte-Carlo calculation (dashed line).

4. - FISSION FRAGMENT DETECTION AND EXPERIMENTAL PROCEDURE.

The fission experiments are performed by detecting the fragments by means of solid state track-detectors (SSTD).

For fission cross-section measurements, a thin target of the sample and a detector strip are tightened together in order to ensure a complete surface contact in such a way to obtain a 2π-geometry.

TABLE II - Critical angles θ_c and detection efficiencies in 2π-geometry of various solid state track detectors for fission fragments.

Detectors	θ_c	Detection efficiency
Soda-lime glass	35°30'	42.6%
Mica	4°30'	91.8%
Macrofol (Bayer)	3°	95.2%

The various types of track detectors have a "critical angle" θ_c, defined between the fragment direction and the detector surface. For fragments impinging the detector surface with an angle $\theta < \theta_c$ the tracks fail to register. Consequently the various SSTD have a different detection efficiency[19]. The values of θ_c and the corresponding efficiencies in "2π-geometry" for some SSTD are collected in Table II. The data are from ref. (19).

Among the various track detectors, we have choosed the mica and the macrofol (Bayer) as they are found to have a very high efficiency and they are also obtainable in very thin layers. This enable us to irradiate simultaneously several target-detector pairs without to sensitively degrade the spectrum of the γ-ray beam. The selected detectors are able to withstand high exposure doses of photons and, also, to discriminate fission tracks against high background of less ionising radiations as, for instance, γ-rays and α-particles.

After the exposure, the detector layers are etched by an appropriate chemical solution and the fission tracks are counted under an optical microscope.

In order to obtain the absolute values of the fission cross-section, thin targets of known thickness are required. In the present experiment the targets are prepared depositing by thermal evaporation a layer of the sample onto very thin Al plates. The thickness and the uniformity of each layer are measured by an optical interferometer and by the charged particle backscattering technique. The first method, which requires an appropriate evaporation technique[20], allows us only to measure the layer thickness with an experimental accuracy of ± 0.005 μm. The second one, described in detail in ref. (21), gives directly the number of atoms per cm^2 of the sample with an experimental accuracy better than 5%.

A cylindrical chamber placed co-axially with the photon beam direction is used for the measurements of the angular and azimuthal distributions of the fission fragments. A detector foil (mica or macrofol) covers the internal wall of the cylinder and the target of the sample is mounted on the base of the chamber, as shown in Fig. 6.

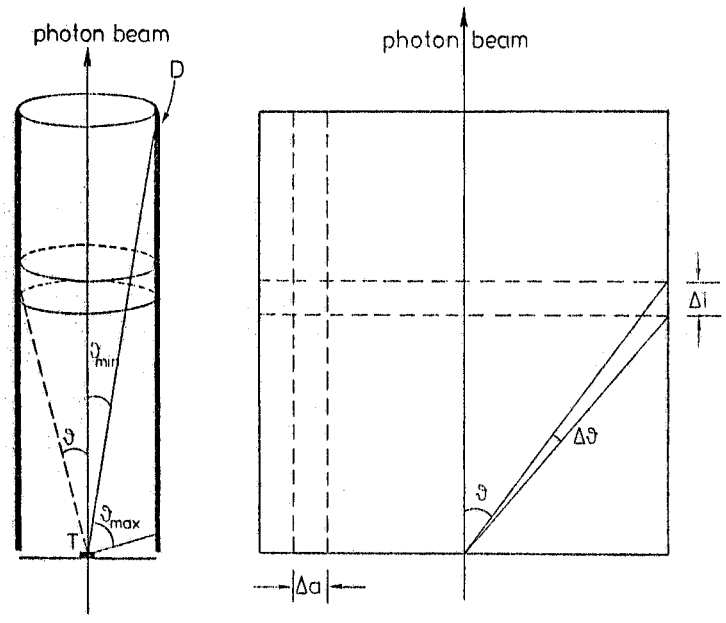

FIG. 6 - Schematic diagram of the track registration geometry used for the angular and azimuthal distribution measurements. T = fissioning target ; D = SSTD foil. The right-hand drawing illustrates the position of the detector foil during irradiation. The left-hand drawing shows the unfolded detector foil.

This cylindrical chamber allows us to obtain simultaneously the angular distributions at various azimuthal angles φ and the azimuthal distributions at various emission angles θ by means of only one irradiation at a fixed photon energy.

In fact, by measuring the track density (number of fission events per surface unit) registred

in a "vertical" strip of width Δa, along the cylinder axis, we obtain the fragment distribution against the angle θ of emission with respect to the photon beam direction, at a fixed value of the azimuthal angle $\varphi \pm \Delta\varphi$. This is the angular distribution $W(\theta, \varphi_{fixed})$. An other strip of detector, symmetric to the first one with respect to the photon beam, gives an identical information.

The measurements, moreover, of the fission track density registred in a "horizontal" strip of width Δl, at a distance r from the line base of the cylinder, allows us to deduce the fragment distribution against the azimuthal angle φ at a fixed emission angle $\theta \pm \Delta\theta$. This is the azimuthal distribution $W(\theta_{fixed}, \varphi)$.

The Fig. 6 show the track registration geometry used for the fragment distribution measurements. By using a cylindrical chamber of radius R = 2 cm and length L = 20 cm, we can measure angular distribution between $\theta_{min} \simeq 6^o$ and $\theta_{max} \simeq 80^o$, with respect to the photon direction. The values θ_{max} depend not only on the geometrical arrangement of the chamber but also on the thickness of the fissioning sample because of the effects of the fragment absorption in crossing the target.

In order to neglect the loss of fragments due to the absorption, the thickness s of the target must satisfy the following condition:

$$\frac{s}{\cos \theta_{max}} \leq \bar{\varrho} \qquad (5)$$

where $\bar{\varrho}$ is the shortest range of the fission fragments in the sample.

In the case of ^{238}U, being $\bar{\varrho} \simeq 8$ mg/cm^2 (ref. (22, 23)), the target thickness must be $s \leq 1.4$ mg/cm^2, if one wants to detect fission fragments also emitted at $\theta_{max} \simeq 80^o$ with respect to the photon beam.

The experimental set-up drawn in Fig. 7 allows us to perform simultaneously the measurements of the fragment distributions and of the cross-section.

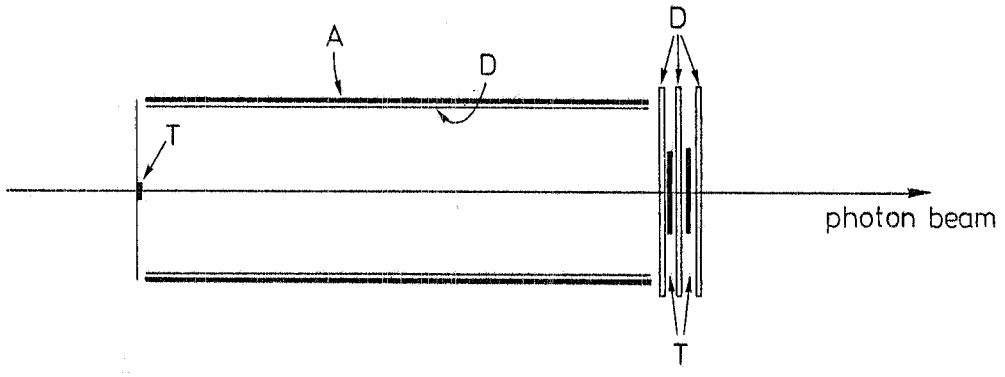

FIG. 7 - Experimental set-up to perform simultaneously measurements of fission fragment distributions and of cross-sections. A = cylindrical chamber; D = SSTD foil; T = target.

In this condition, the outher surface of the first detector of the stack collected also the fission fragments emitted at $\theta = 0^o$ from the target placed on the base of the cylindrical chamber.

APPENDIX.

In order to show the improvement in the information on the fission channels that can be attained by using polarized photons also in the case where only three channels are excited, we have performed a numerical simulation. We have assumed the experimental data of the fission fragment angular distribution obtained for $E_\gamma = 7.38$ MeV and $P = 0$ by Dowdy and Krysinski[11]. The experimental points and their errors have been deduced by Fig. 3 of ref. (11) and are plotted in Fig. 8 (closed circles).

From the least-square fit of these experimental points (dashed curve of Fig. 8), we have obtained the a, b and c coefficients and then, solving the first three equations of the system (4) for $P = 0$, we have estimated the three unknowns $\sigma_{0,2}$, $\sigma_{0,1}$ and $\sigma_{1,1}$. The obtained values are reported in the first column of Table III.

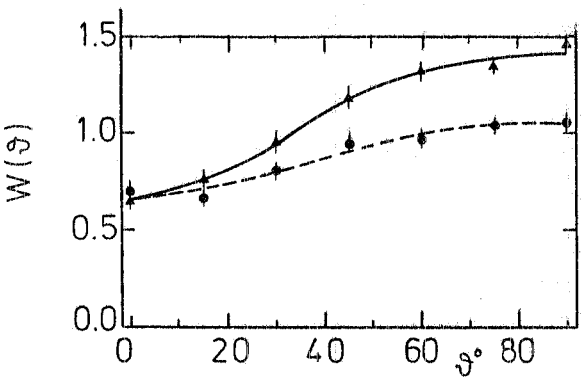

FIG. 8 - Fragment angular distribution $W(\theta)$ in ^{238}U photofission at $E_\gamma = 7.38$ MeV. Experimental points: ● data from ref. (11); ▲ data evaluated by us (see text). The dashed curve represents the least-square fit in the case $P = 0$, the continuous one is the best fit for $P = 1$.

TABLE III - Values of the partial cross-section $\sigma_{K,J}$ for photofission through the corresponding channel (K, J). Arbitrary units.

	P = 0	P = 1
$\sigma_{0,2}$	0.025 ± 0.019	0.036 ± 0.009
$\sigma_{0,1}$	0.473 ± 0.025	0.461 ± 0.011
$\sigma_{1,1}$	0.452 ± 0.017	0.436 ± 0.011

Starting from these values of $\sigma_{0,2}$, $\sigma_{0,1}$ and $\sigma_{1,1}$, we have evaluated the angular distribution $W(\theta, \pi/2)$, expected in the case $P = 1$.

Then a set of errors, extracted by a gaussian population with a relative standard deviation equal to that of the initial experimental data, have been added to the obtained points. So we have got the data reported in Fig. 8 as closed triangles. In the same figure the continuous curve represents the least-square fit from which we have deduced the a, b and c coefficients and their errors.

Solving the first three equations of the system (4) in the case $P = 1$, we have estimated the $\sigma_{0,2}$, $\sigma_{0,1}$ and $\sigma_{1,1}$ unknowns, reported in the second column of Table III.

From Table III we note that the values of the partial cross-sections agree within the experimental errors in the two cases, but the errors on the cross-sections obtained for $P = 1$ are lower than the ones for $P = 0$. A strong improvement is obtained particularly in the estimate of the $(0, 2^+)$ contribution.

REFERENCES.

(1) - G. C. Baldwin and G. S. Klaiber, Phys. Rev. 71, 3 (1947).

(2) - R. B. Duffield and J. R. Huizenga, Phys. Rev. 89, 1024 (1953).

(3) - J. E. Gindler and J. R. Huizenga, Phys. Rev. 104, 425 (1956).

(4) - L. Katz, A. P. Baerg and F. Brown, Proc. of the Second Intern. Conf. on Peaceful Uses of Atomic Energy, Geneva 1958 (United Nations, 1958), vol. 15, p. 188.

(5) - N. S. Rabotnov, G. N. Smirenkin, A. S. Soldatov, L. N. Usachev, S. P. Kapitza and Yu. M. Tsipenyuk, Sov. J. Nucl. Phys. 11, 285 (1970).

(6) - A. V. Ignatyuk, N. S. Rabotnov, G. N. Smirenkin, A. S. Soldatov and Yu. M. Tsipenyuk, JETP 34, 684 (1974).

(7) - C. D. Bowman, I. G. Schroder, C. E. Dick and H. E. Jackson, Phys. Rev. C12, 863 (1975).

(8) - V. E. Zhuchko, A. V. Ignatyuk, Yu. B. Ostapenko, G. N. Smirenkin, A. S. Soldatov and Yu. M. Tsipenyuk, Phys. Letters 68B, 323 (1977).

(9) - L. J. Lindgren, A. Alm and A. Sandell, Nuclear Phys. A298, 43 (1978).

(10) - A. Manfredini, L. Fiore, C. Ramorino, H. G. De Carvalho and W. Wolfli, Nuclear Phys. A127, 637 (1969), and references therein.

(11) - E. J. Dowdy and A. Krysinski, Nuclear Phys. A175, 501 (1971).

(12) - O. Y. Mafra, M. F. Cesar, C. Renner and J. Goldemberg, Nuclear Phys. A236, 1 (1974).

(13) - T. Dragnev, E. Dermendjiev, N. Kalinkova, N. Kashukeev, N. Tschikov and N. Yaneva, Progress Report on Nuclear Data Activities in Bulgaria, 1973, p. 42.

(14) - J. T. Caldwell, E. J. Dowdy, B. L. Berman, R. A. Alvarez and P. Meyer, Phys. Rev. C21, 1215 (1980), and references therein.

(15) - J. D. T. Arruda Neto, S. B. Herdabe, B. S. Bhandari and I. C. Nascimento, Nuclear Phys. A334, 297 (1980).

(16) - V. Bellini, M. Di Toro, S. Lo Nigro and G. S. Pappalardo, Lett. Nuovo Cimento 26, 173 (1980).

(17) - L. Federici, G. Giordano, G. Matone, G. Pasquariello, P. G. Picozza, R. Caloi, L. Casano, M. P. De Pascale, M. Mattioli, E. Poldi, C. Schaerf, M. Vanni, P. Pelfer, D. Prosperi, S. Frullani and B. Girolami, Nuovo Cimento 59B, 247 (1980).

(18) - J. A. Wheeler, in Fast Neutron Physics, ed. by J. B. Marion and J. L. Fowler (Wiley-Interscience, 1963), part II.

(19) - H. A. Khan and S. A. Durrani, Nuclear Instr. and Meth. 98, 229 (1972).

(20) - V. Emma and S. Lo Nigro, Nuclear Instr. and Meth. 128, 355 (1975).

(21) - G. Foti, J. W. Mayer and E. Rimini, in Ion Beam Handbook for Material Analysis, ed. by J. W. Mayer and E. Rimini (Academic Press, 1977), chap. II, p. 21.

(22) - J. B. Niday, Phys. Rev. 121, 1471 (1961).

(23) - H. Farrar and R. H. Tomlinson, Nuclear Phys. 34, 367 (1962).